Original Research

Quercetin protects macrophages from oxidized low-density lipoprotein-induced apoptosis by inhibiting the endoplasmic reticulum stress-C/EBP homologous protein pathway

Shutong Yao[1,2], Hui Sang[1,2], Guohua Song[1], Nana Yang[1], Qinghua Liu[3], Ying Zhang[1], Peng Jiao[1], Chuanlong Zong[1] and Shucun Qin[1,2]

[1]Institute of Atherosclerosis, Key Laboratory of Atherosclerosis in University of Shandong; [2]College of Basic Medical Sciences, Taishan Medical University; [3]Department of Clinical Laboratory, Affiliated Hospital of Taishan Medical University, Taian, Shandong 271000, China

Corresponding author: Shucun Qin. Email: shucunqin@hotmail.com

Abstract

Quercetin (QUE), a member of the bioflavonoid family, has been proposed to have antioxidative, anti-inflammatory and antihypertensive properties. This study was designed to investigate the protective effect of QUE on oxidized low-density lipoprotein (ox-LDL)-induced cytotoxicity in RAW264.7 macrophages and specifically the endoplasmic reticulum (ER) stress-C/EBP homologous protein (CHOP) pathway-mediated apoptosis. Our results showed that treatment with QUE (20, 40 and 80 μmol/L) significantly attenuated ox-LDL-induced cholesterol accumulation in macrophages and foam cell formation in a dose-dependent manner. Similar to tunicamycin (TM), a classical ER stress inducer, ox-LDL reduced cell viability and induced apoptosis in RAW264.7 macrophages. The cytotoxic effects of ox-LDL and TM were significantly inhibited by QUE treatment. Interestingly, we found that QUE also significantly suppressed the ox-LDL- and TM-induced activation of ER stress signaling events, including the phosphorylation of inositol-requiring enzyme 1 (IRE1), translocation of activating transcription factor 6 (ATF6) from the cytoplasm to the nucleus and upregulation of X-box-binding protein 1. In addition, exposure of RAW264.7 macrophages to ox-LDL or TM resulted in a significant increase in the expression of CHOP, a transcription factor regulated by IRE1 and ATF6 under conditions of ER stress, as well as a decrease in Bcl-2 transcript and protein concentrations. QUE blocked these effects in a dose-dependent manner. These data indicate that QUE can protect RAW264.7 cells from ox-LDL-induced apoptosis and that the mechanism at least partially involves its ability to inhibit the ER stress-CHOP signaling pathway.

Keywords: quercetin, endoplasmic reticulum stress, CHOP, ox-LDL, macrophage, apoptosis

Experimental Biology and Medicine 2012; **237**: 822–831. DOI: 10.1258/ebm.2012.012027

Introduction

Atherosclerotic plaque rupture is the precipitating event that results in the majority of clinical manifestations of acute coronary syndrome patients, including unstable angina, acute myocardial infarction and sudden coronary death.[1] There is increasing evidence that macrophages are intimately involved in the formation and destabilization of atherosclerotic plaques.[2,3] It is now believed that apoptosis of lipid-containing macrophages initially contributes to the lipid core formation and later to plaque instability.[4] Indeed, macrophage apoptosis occurs during all stages of atherosclerosis. In early lesions, the process of phagocytic clearance of apoptotic macrophages is efficient, decreases macrophage burden, limits lesion cellularity and suppresses plaque progression.[5] However, in advanced lesions, where this process is defective, macrophage apoptosis promotes an inflammatory response and lesional necrosis, which lead to plaque disruption and acute thrombosis.[2–4] Thus, reducing macrophage apoptosis in late lesions is an attractive strategy for attenuating plaque instability.[2,6]

Quercetin (QUE; 3,3′,4′,5,7-pentahydroxylflavone) is one of the well-studied flavonoids that are ubiquitous in plants and are present in considerable amounts in fruits and vegetables.[7] QUE has been reported to have physiological functions such as antioxidative activity,[8] lowering of blood pressure[9] and ameliorating hyperglycemia-related diseases.[10] The antiapoptotic effects of QUE have been reported in several cells such as neural cells, cardiomyoblast cells and endothelial cells.[11–13] Chow *et al.*[14] have shown

that QUE inhibits H_2O_2-induced macrophage apoptosis via its antioxidant activity and by modulating heme oxygenase 1 gene expression. However, the relationship between the endoplasmic reticulum (ER) stress-C/EBP homologous protein (CHOP) pathway and prevention of macrophage-derived foam cell apoptosis by QUE is still unknown.

CHOP, also known as growth arrest and DNA damage-inducible gene 153 (GADD153), is a leucine zipper transcription factor that is present at low levels under normal conditions but is robustly expressed in response to ER stress.[15] CHOP deficiency has been shown to attenuate myocardial reperfusion injury by inhibiting myocardial apoptosis and inflammation.[16] Mice deficient in CHOP are also markedly protected from pancreatic β-cell apoptosis and diabetes.[17] Recently, ER stress-CHOP pathway-mediated apoptosis in macrophages has been demonstrated to contribute to the instability of atherosclerotic plaques, and CHOP deficiency has been found to protect macrophages from ER stress-induced apoptosis *in vitro* and in advanced atherosclerotic lesions of mice.[18–21] Thus, there is a positive correlation among CHOP expression, apoptosis of macrophage cells and progression of atherosclerotic plaques to the vulnerable stage.[22]

Oxidized low-density lipoprotein (ox-LDL) plays an important role in the formation of foam cells, and induces macrophage apoptosis.[23] We have previously shown that ox-LDL can induce ER stress during the formation of macrophage-derived foam cells.[24] However, if QUE protects macrophages from ox-LDL-induced apoptosis by inhibiting the ER stress-CHOP pathway remains unclear. In this study, we investigated the link between ox-LDL-induced apoptosis and activation of the ER stress pathway using RAW264.7 macrophages. Furthermore, we provide evidence for the anti-apoptotic effect of QUE, with emphasis on its role in downregulating the ER stress-CHOP pathway-mediated apoptosis.

Materials and methods

Reagents

QUE, tunicamycin (TM), oil red O and rabbit antibody against β-actin were obtained from Sigma (St Louis, MO, USA). Dulbecco's modified Eagle's medium (DMEM) and fetal bovine serum were purchased from Gibco (BRL, Gaithersburg, MD, USA). RIPA lysis buffer and bicinchoninic acid (BCA) protein quantitation kits were purchased from Solarbio (Beijing, China). Rabbit polyclonal antibodies against CHOP and Bcl-2 were purchased from Santa Cruz Biotechnology (Santa Cruz, CA, USA). Rabbit antibodies against activating transcription factor 6 (ATF6), phosphoinositol-requiring enzyme 1 (p-IRE1) and X-box-binding protein 1 (XBP1) were purchased from Abcam (Cambridge, MA, USA). Horseradish peroxidase-labeled goat anti-rabbit IgG and SABC-Cy3 immunohistochemistry reagent kits were obtained from Boshide (Wuhan, China). 3-(4,5-dimethylthiazol-2-y-l)-2,5-diphenyl-2H-tetrazolium bromide (MTT) was purchased from Genview (Houston, TX, USA). The Annexin V-FITC apoptosis detection kit was purchased from KeyGEN Biotech (Nanjing, China). Polyvinylidene fluoride (PVDF) membranes were purchased from Millipore (Bedford, MA, USA). Enhanced chemiluminescence (ECL) kits were purchased from Thermo Scientific Pierce (Rockford, IL, USA). Realtime polymerase chain reaction (PCR) reagent kits were purchased from Tiangen Biological Chemistry (Beijing, China) and tissue/cell free cholesterol assay kits from Applygen (Beijing, China).

Isolation and oxidation of LDL

Human LDL was isolated and oxidized as described recently.[25] In brief, LDL (density = 1.019–1.063 g/mL) was isolated from plasma of normolipidemic donors by sequential ultracentrifugation, and incubated with 10 μmol/L $CuSO_4$ for 18 h at 37°C. Following incubation, 0.1 mmol/L ethylenediaminetetraacetic acid (EDTA) was added to prevent further oxidation, and the oxidized LDL was concentrated to 1 mg/mL. The extent of LDL oxidation was assessed based on its increased mobility in an agarose gel (compared with that of native LDL) and also by the presence of increased concentrations of thiobarbituric acid-reactive substances (TBARS) in the sample. Typically, ox-LDL preparations had TBARS of >30 μmol/g protein and a relative mobility index on agarose gels of 2.0–2.5 when compared with that of native LDL. Lipoproteins were stored at 4°C in the dark and freshly prepared every two weeks.

Cell culture and treatment

RAW264.7, a mouse macrophage cell line, was purchased from the Type Culture Collection of the Chinese Academy of Sciences (Shanghai, China). Cells were cultured in DMEM supplemented with 2 mmol/L glutamine, antibiotics (100 U/mL penicillin A and 100 U/mL streptomycin) and 10% heat-inactivated fetal bovine serum, and maintained in a 37°C humidified incubator containing 5% CO_2.

RAW264.7 cells were treated with 100 mg/L of ox-LDL for 24 h or 5 mg/L of TM (a classical ER stress inducer) for 12 h in the presence or absence of different concentrations of QUE.

Oil red O staining for the detection of cytoplasmic lipids

Cells were cultured on glass coverslips in six-well plates and incubated with 100 mg/L ox-LDL for 24 h in the presence or absence of QUE. Cells were washed with phosphate-buffered saline (PBS), fixed with a 4% paraformaldehyde solution for 20 min, stained with 0.5% oil red O in isopropanol for 30 min, and counterstained with hematoxylin for another five minutes. The cells were visualized using an Olympus BX51 microscope (Olympus, Tokyo, Japan), and the images were recorded with a JVC 3-CCD camera (Olympus) and analyzed using Image-Pro Plus software (version 6.0; Media Cybernetics, Bethesda, MD, USA). The lipid droplet content was expressed as the average value of the integrated optical density.

Intracellular total cholesterol assay

The intracellular total cholesterol (TC) concentration was measured using a tissue/cell TC assay kit according to the manufacturer's instructions. RAW264.7 cells were treated

as described above and then harvested and divided into two equal portions to be processed for measurement of protein concentration and TC content. Lipids were extracted using a lysis solution provided in the kit. To determine TC concentrations, cholesterol ester hydrolase was used to convert cholesterol ester into free cholesterol. Then, cholesterol oxidase was used to generate H_2O_2 from the free cholesterol generated in the previous step, and peroxidase was used to catalyze the reaction of H_2O_2 with 4-amino-antipyrine and phenol to yield a stable rose-color product. The absorbance of this colored product was measured at 550 nm using an Infinite F200 microplate reader (Tecan, Männedorf Switzerland), and the concentration of TC was determined using a standard curve and was normalized to levels of total cellular protein.

MTT assay

Cell viability was determined using the MTT reduction assay. Briefly, cells were seeded at a density of 1×10^4 cells/well in 96-well plates and were treated with 100 mg/L of ox-LDL for 24 h or with 5 mg/L of TM for 12 h in the presence or absence of QUE. Following the incubations, MTT was added to a final concentration of 0.5 mg/mL and the samples were incubated at 37°C for four hours. After removing the supernatant, 150 μL dimethylsulfoxide was added to dissolve the formazan crystals, and the optical density was measured at 490 nm using an Infinite F200 microplate reader (Tecan). Cell viability was expressed as the percentage of the MTT count of treated cells relative to that of the untreated control cells (100%).

Detection of apoptosis by flow cytometry analysis and laser scanning confocal microscopy

The Annexin V-FITC/PI double-staining assay was used to quantify apoptosis according to the manufacturer's protocol. Following treatment, cells were centrifuged, washed with PBS and resuspended in 500 μL binding buffer, and incubated with 5 μL Annexin V-FITC and 5 μL of propidium iodide (PI) solution for 10 min at room temperature in the dark. The samples were analyzed on a FACScan flow cytometer using CellQuest software (Becton Dickinson, San Jose, CA, USA). Double staining of cells with Annexin V-FITC and PI allowed the identification of different cell populations based on their staining patterns as follows: live cells ($FITC^-PI^-$), early apoptotic ($FITC^+PI^-$), late apoptotic ($FITC^+PI^+$) and necrotic cells ($FITC^-PI^+$).

The cells treated as described above were analyzed on glass coverslips using a laser scanning confocal microscope (Bio-Rad Radiance 2100, Hercules, CA, USA) with 488 nm excitation and 525 nm emission wavelengths. Cells undergoing prophase apoptosis fluoresced bright green fluorescence due to Annexin V-FITC staining, whereas the nuclei of cells undergoing advanced stage apoptosis fluoresced cardinal red due to PI staining.

Immunofluorescence assay for ATF6 nuclear relocation

RAW264.7 cells were grown on glass coverslips until subconfluent. The treated cells were washed with PBS, fixed in 4% paraformaldehyde in PBS, permeabilized with 0.1% Triton-X 100 and blocked in 3% bovine serum albumin (BSA). Samples were incubated with ATF6 antibody (1:100 in PBS–1% BSA) for one hour at room temperature. Following incubation with the appropriate secondary antibody (1:200 in PBS–1% BSA), the samples were incubated with SABC–Cy3 complex and 4′,6-diamidino-2-phenylindole. Coverslips were then washed with PBS and mounted in antifade reagent. Stained cells were analyzed using a laser scanning confocal microscope (Bio-Rad Radiance 2100).

Western blot analysis

Total protein was extracted in RIPA lysis buffer (50 mmol/L HEPES, pH 7.4, 150 mmol/L NaCl, 1% Triton X-100, 4 mmol/L sodium orthovanadate, 20 mmol/L sodium pyrophosphate, 200 mmol/L sodium fluoride, 2 mmol/L phenylmethylsulfonyl fluoride, 1 mmol/L EDTA, 10% glycerol and protease inhibitors), and the insoluble material was removed by centrifugation at 12,000 $\times$ g for 30 min at 4°C. The protein concentration of the supernatant was determined using the BCA protein assay. Equivalent amounts of protein from each lysate sample were mixed with protein loading buffer, heated at 95°C for five minutes, resolved by 8–10% sodium dodecyl sulfate polyacrylamide gel electrophoresis and transferred onto PVDF membranes by electroblotting. After blocking in Tris-buffered saline (TBS) containing 0.1% Tween 20 and 10% non-fat dried milk for two hours at room temperature, the membranes were incubated with primary antibodies for three hours at room temperature or overnight at 4°C. After four washes with TBS containing 0.1% Tween 20, the membranes were incubated with horseradish peroxidase-conjugated secondary antibodies for one hour at room temperature. Protein bands were visualized by ECL reaction. The Image-Pro Plus software was used to measure the band intensities, which were normalized to β-actin protein concentrations.

Quantitative realtime PCR analysis

The Primer Design 4.1 software (Sci-ed Software, Durham, NC, USA) was used to design the following primers: CHOP forward primer: 5′ CCACCACA CCTGAAAGCAGAA 3′, reverse primer: 5′ GGTGCCCCC AATTTCATCT 3′(length of 150 bp); Bcl-2 forward primer: 5′ GGATGACTTCTCTCGTCGCTAC 3′, reverse primer: 5′ TGACATCTCCCTGTTGACGCT 3′ (length of 199 bp); β-actin forward primer: 5′ CGGGGACCTGACTGACTACC 3′, reverse primer: 5′ AGGAAGGCTGGAAGAGTGC 3′ (length of 251 bp). The primers were synthesized by Takara (Shiga, Japan). Total RNA was extracted using Trizol reagent (Invitrogen, Carlsbad, CA, USA) following the manufacturer's instructions. First-strand cDNA was synthesized using MuLV Reverse Transcriptase (Applied Biosystems, Carlsbad, CA, USA) from 2 μg of total RNA. Realtime PCR was performed with a Rotor-Gene Q realtime PCR cycler (Qiagen, Shanghai, China) using SYBR-green PCR master mix kits (TianGen Biotech, Beijing, China). Initial denaturation was performed at 94°C for 10 min,

followed by 40 cycles of denaturation at 94°C for 20 s, then annealing at 56°C for 30 s and extension at 68°C for 30 s. The data were analyzed using the Rotor-Gene Q software (version 1.7; Qiagen), and relative mRNA levels were calculated using the $2^{-\Delta\Delta Ct}$ method and normalized against β-actin. Each experiment was repeated three times.

Statistical analysis

Results are shown as the mean ± SEM for at least three independent experiments. Statistical analysis was performed using one-way analysis of variance (ANOVA) followed by Student–Newmann–Keuls multiple comparison tests with SPSS 13.0 software for Windows (Apache Software Foundation, SPSS Inc., Chicago, IL, USA). P values <0.05 were considered statistically significant.

Results

QUE inhibits ox-LDL-induced lipid accumulation in RAW264.7 cells

The oil red O staining for analysis of lipid droplets indicated that many lipid droplets were present in RAW264.7 cells treated with ox-LDL (100 mg/L) for 24 h. However, the ox-LDL-induced accumulation of lipid droplets was attenuated by QUE in a dose-dependent manner (Figure 1a and b).

Lipid accumulation was further confirmed by intracellular TC quantitative assay. Compared with the control, intracellular TC content was significantly increased (2.7-fold) by ox-LDL treatment (100 mg/L) for 24 h. This effect was attenuated by 20.4%, 29.4% and 40.9% upon QUE treatment at 20, 40 and 80 μmol/L, respectively (Figure 1c).

QUE protects RAW264.7 cells from cell death induced by ox-LDL or TM

The cytotoxic effect of QUE in RAW264.7 cells was evaluated by MTT assay. Our results indicated that treatment with QUE at 20, 40 and 80 μmol/L for 24 h did not result in a significant reduction in cellular viability (Figure 2a). Next, we determined the protective effect of QUE on ox-LDL-induced cell death. The addition of ox-LDL at 100 mg/L for 24 h decreased cell viability by approximately 52.4% as measured by MTT assay. However, incubation of ox-LDL-treated cells with different doses of QUE (20, 40 and 80 μmol/L) resulted in a dose-dependent increase in cell viability (23.9%, 49.6%, and 66.9%, respectively) compared with cells not treated with QUE (Figure 2b).

To determine the protective effect of QUE on ER stress-mediated cell death, TM, a classical ER stress inducer, was used in the study. As illustrated in Figure 2c, when RAW264.7 cells were treated with both QUE (80 μmol/L) and TM (5 mg/L) for 12 h, cell viability increased compared with TM treatment alone. This suggested that QUE was able to inhibit ER stress-induced reduction in cellular viability.

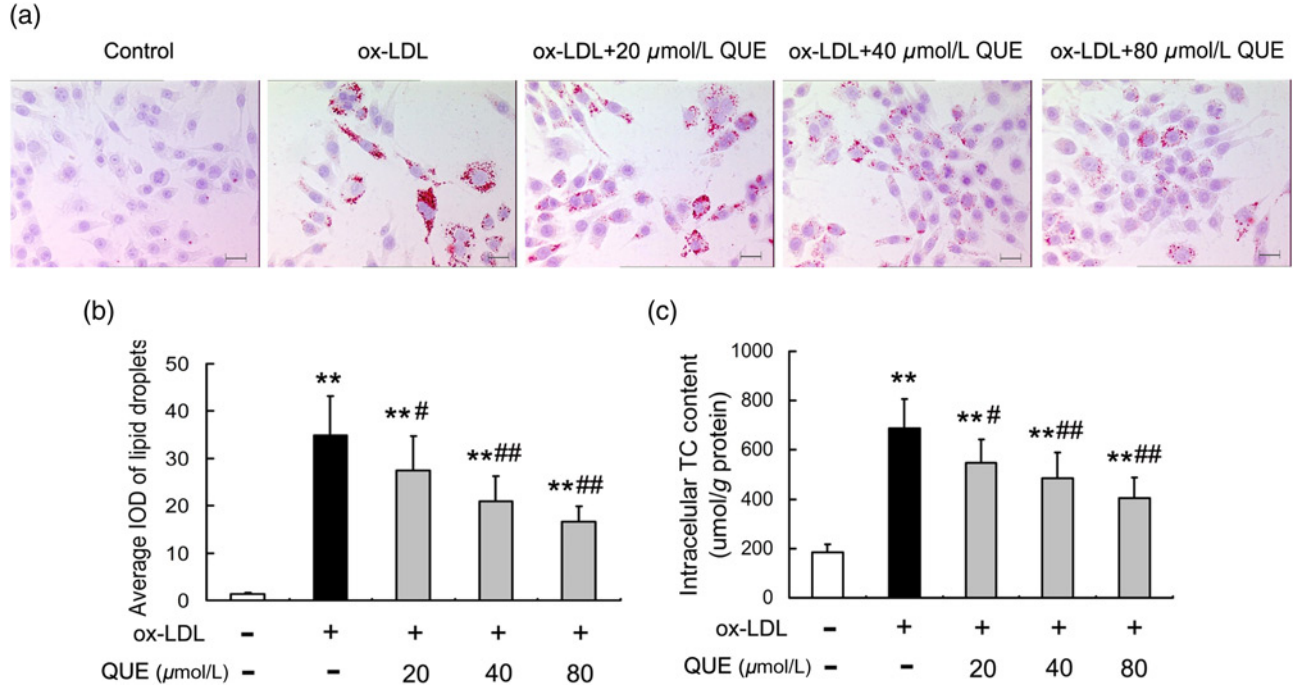

Figure 1 QUE reduces ox-LDL-induced intracellular lipid accumulation in RAW264.7 cells. (a) Cells were treated with ox-LDL (100 mg/L) in the absence or presence of QUE at different concentrations (20, 40 and 80 μmol/L) for 24 h, and the intracellular lipid droplets were stained by oil red O. Representative lipid droplet staining images are shown. Scale bar = 20 μm. (b) The average integrated optical density (IOD) of lipid droplets stained with oil red O from differentiated macrophage foam cells was obtained via checking five fields in each condition. (c) Under the same conditions as in (a), the intracellular total cholesterol (TC) content was measured using a tissue/cell TC assay kit. Data are presented as the mean ± SEM of at least four independent experiments. $^{**}P < 0.01$ versus vehicle-treated control; $^{\#}P < 0.05$, $^{\#\#}P < 0.01$ versus ox-LDL treatment. QUE, quercetin; ox-LDL; oxidized LDL. (A color version of this figure is available in the online journal)

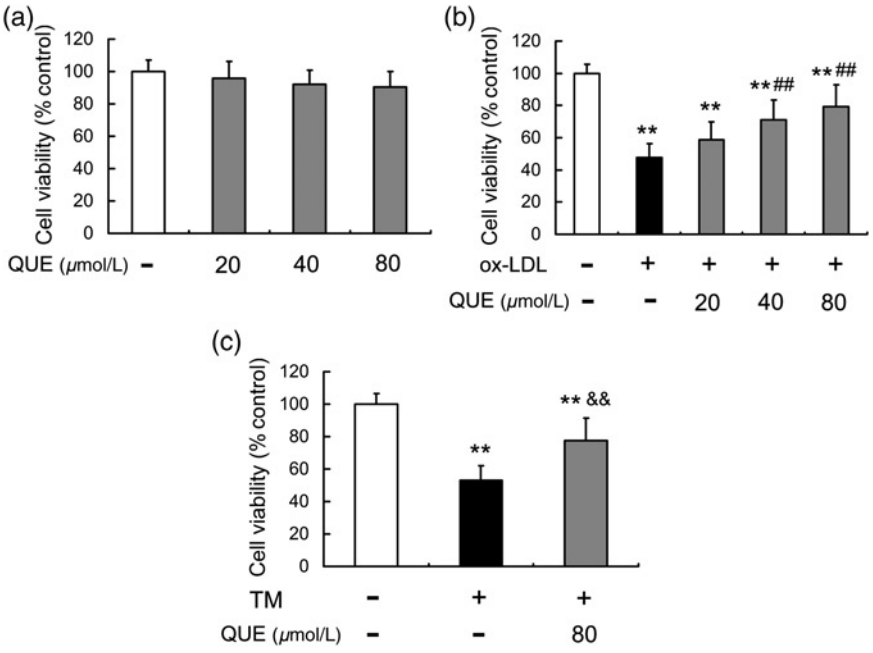

Figure 2 Effects of QUE on cell viability. (a) Determination of the cytotoxic effects of QUE on RAW264.7 cells. Cells were treated with different concentrations (20, 40 and 80 μmol/L) of QUE for 24 h. (b) QUE inhibits ox-LDL-induced cell death. Cells were treated with different concentrations (20, 40 and 80 μmol/L) of QUE in the presence of ox-LDL (100 mg/L) treatment for 24 h. (c) QUE inhibits tunicamycin (TM)-induced cell death. Cells were treated with QUE (80 μmol/L) in the presence of TM (5 mg/L) for 12 h. The viability of cells under different treatments was measured by MTT assay and expressed as the percentage of control (survival of control). Data are expressed as the mean ± SEM of at least three independent experiments. $^{**}P < 0.01$ versus vehicle-treated control; $^{\#\#}P < 0.01$ versus ox-LDL treatment; $^{\&\&}P < 0.01$ versus TM treatment. QUE, quercetin; ox-LDL; oxidized LDL

QUE attenuates ox-LDL- or TM-induced apoptosis of RAW264.7 cells

To determine whether QUE could protect against ox-LDL-induced apoptosis, the treated cells were subjected to Annexin V-FITC/PI double staining and analyzed by flow cytometry. As observed in Figure 3a, the treatment of RAW264.7 cells with 100 mg/L ox-LDL for 24 h induced apoptosis, whereas QUE treatment (20, 40 and 80 μmol/L) reduced ox-LDL-induced apoptosis in a dose-dependent manner.

Morphological changes in cells were also observed using laser scanning confocal microscopy after Annexin V-FITC/PI staining of the cells. As shown in Figure 3b, typical morphological changes, such as PI staining throughout the nuclei and a halo of bright green staining (Annexin V-FITC) on the plasma membrane, appeared when cells were treated with 100 mg/L of ox-LDL for 24 h. In contrast, QUE-treated cells did not show these evident morphological changes associated with apoptosis.

A similar anti-apoptotic activity of QUE was also observed in a TM-induced apoptosis model. Flow cytometry analysis showed that the increase in apoptotic rate induced by TM was inhibited by the addition of QUE (Figure 3c).

Effect of QUE on the expression of CHOP and Bcl-2

CHOP is involved in the process of apoptosis associated with ER stress through mechanisms that involve down-regulation of Bcl-2.[26] To determine the effect of QUE on ox-LDL-induced CHOP and Bcl-2 expression, a Western blot assay was performed as described in the Materials and methods section. Ox-LDL treatment resulted in a significant increase in CHOP expression in RAW264.7 cells (63.5-fold), while Bcl-2 protein expression decreased by 75.0%, compared with untreated control cells. However, treatment of cells with 20, 40 and 80 μmol/L QUE decreased CHOP levels by 27.6%, 41.9% and 61.9%, respectively, and simultaneously increased Bcl-2 levels by 1.8-, 2.2- and 3.2-fold, respectively, compared with ox-LDL-treated cells (Figure 4a).

The effect of QUE on the ox-LDL-induced modulation of CHOP and Bcl-2 transcript levels was also determined by realtime PCR (Figure 4b). Consistent with the Western blot results, QUE treatment significantly decreased levels of CHOP mRNA and increased Bcl-2 mRNA levels in a dose-dependent manner, compared with that of ox-LDL-treated cells.

In the TM-induced ER stress model, similar effects of QUE on CHOP and Bcl-2 protein and mRNA levels were observed. Treatment of cells with 80 μmol/L QUE decreased CHOP protein and mRNA levels by 36.2% and 32.9%, respectively, and increased Bcl-2 protein and mRNA levels by 134.0% and 84.3%, respectively, compared with TM-treated cells (Figure 4c and d).

QUE inhibits ox-LDL- or TM-mediated activation of ATF6

ER transmembrane-localized p90-ATF6 (the inactive form of ATF6) is cleaved into p50-ATF6, which translocates to the nucleus where it specifically binds to ER stress response element (ERSE) to activate the transcription of CHOP.[27,28]

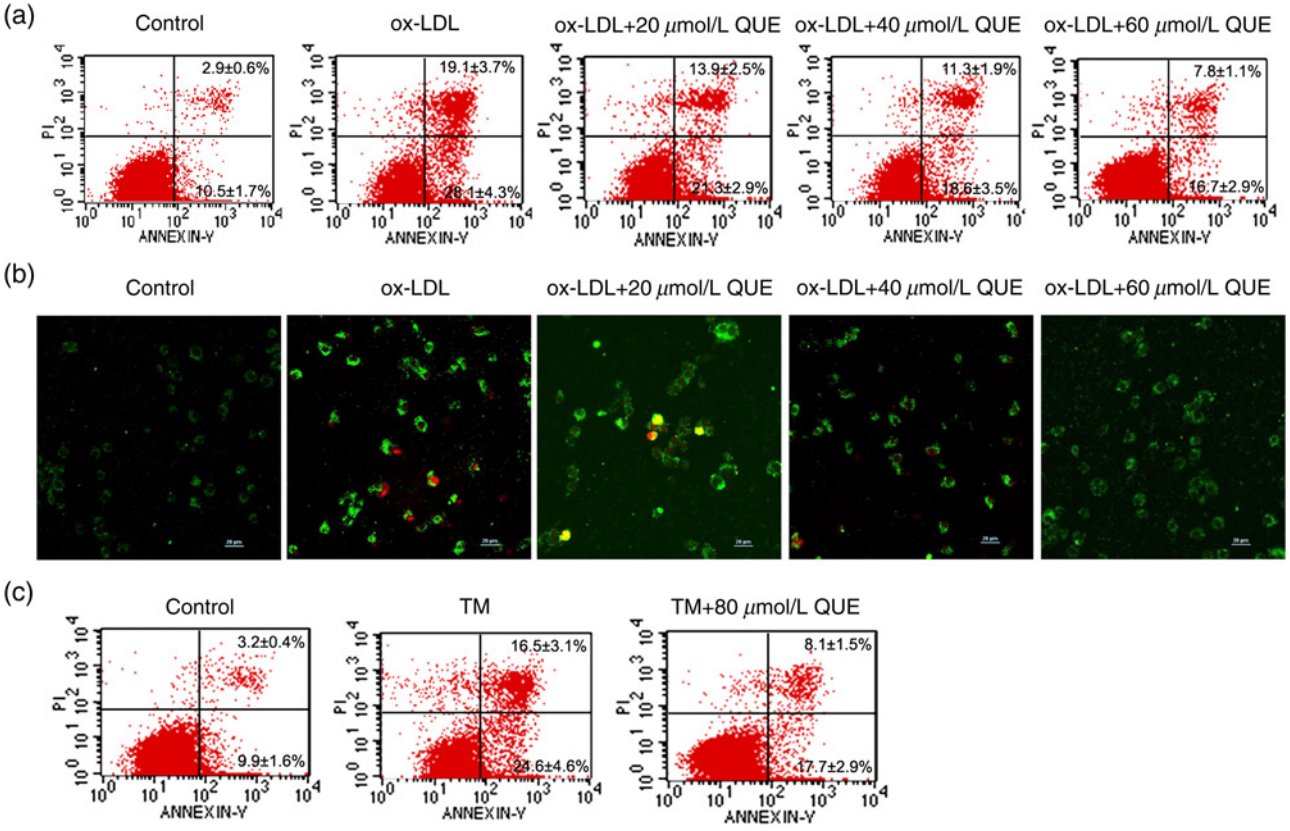

Figure 3 QUE decreases apoptosis induced by ox-LDL or tunicamycin (TM) in RAW264.7 cells. (a) Cells were treated with ox-LDL (100 mg/L) in the absence or presence of QUE at different concentrations (20, 40 and 80 μmol/L) for 24 h, and the population of apoptotic cells stained with Annexin V-FITC and PI was detected by flow cytometry analysis. (b) Cells were treated as described in (a), and the morphological changes of apoptotic cells were observed with laser scanning confocal microscope by AnnexinV-FITC/PI staining. Representative images are shown. Scale bar = 20 μm. (c) Cells were treated with TM (5 mg/L) in the absence or presence of QUE (80 μmol/L) for 12 h, and the ratio of apoptotic cells stained with Annexin V-FITC and PI was detected by flow cytometry analysis. A representative of data of flow cytometry analysis was presented. The percentage of apoptotic cells under different treatments was measured and expressed as the mean $\pm$ SEM from three independent experiments. QUE, quercetin; ox-LDL; oxidized LDL; PI, propidium iodide. (A color version of this figure is available in the online journal)

The induction of CHOP protein and mRNA by ox-LDL or TM (Figure 4) suggests that p90-ATF6 is activated into p50-ATF6. We used immunofluorescence analysis to confirm this hypothesis. As shown in Figure 5, ATF6 showed a diffused cytoplasmic localization in untreated control cells, whereas clusters of ATF6 were detected in the nuclear region in ox-LDL- or TM-treated cells, indicative of activated ATF6. The ATF6 relocation from the cytoplasm to the nucleus in RAW264.7 cells induced by ox-LDL or TM was significantly inhibited by QUE.

Effect of QUE on the expression of p-IRE1 and XBP-1

XBP-1, another transcription factor that positively regulates CHOP transcription through binding to ERSE, is induced by both ATF6 and IRE1.[29,30] The effect of QUE on the expression of p-IRE1 and XBP-1 was examined by immunoblotting analysis. As shown in Figure 6, both p-IRE1 and XBP-1 protein levels were increased in the presence of ox-LDL and TM. However, QUE significantly suppressed the upregulation of p-IRE1 and XBP-1 expression induced by ox-LDL or TM.

Discussion

Apoptosis is a key event in the progression of advanced atherosclerosis. Apoptosis of lipid-containing macrophages leads to the development of the necrotic core in an atherosclerotic plaque and reduced excretion of cellular matrix in the plaque region. This is a contributing factor in plaque instability that then results in a number of cardiovascular complications.[31] Thus, suppression of macrophage apoptosis may be effective in preventing acute cardiovascular events. Considerable efforts have been made to identify a natural compound that has cardiovascular benefits. QUE, one of the flavonoids that is ubiquitous in plants, was reported to demonstrate antiapoptotic properties in various cell types.[11–14] Nevertheless, the effect of QUE on ox-LDL-induced macrophage apoptosis and the possible molecular mechanisms of its physiological effects remained to be elucidated. The results of this study suggest that QUE prevents ox-LDL-induced apoptosis in macrophages and suppresses the ER stress-CHOP pathway via inhibiting ATF6 and IRE1 activation. Moreover, QUE results in reduced CHOP expression with an increase in Bcl-2 gene expression, which could potentially be a cyto-protective mechanism.

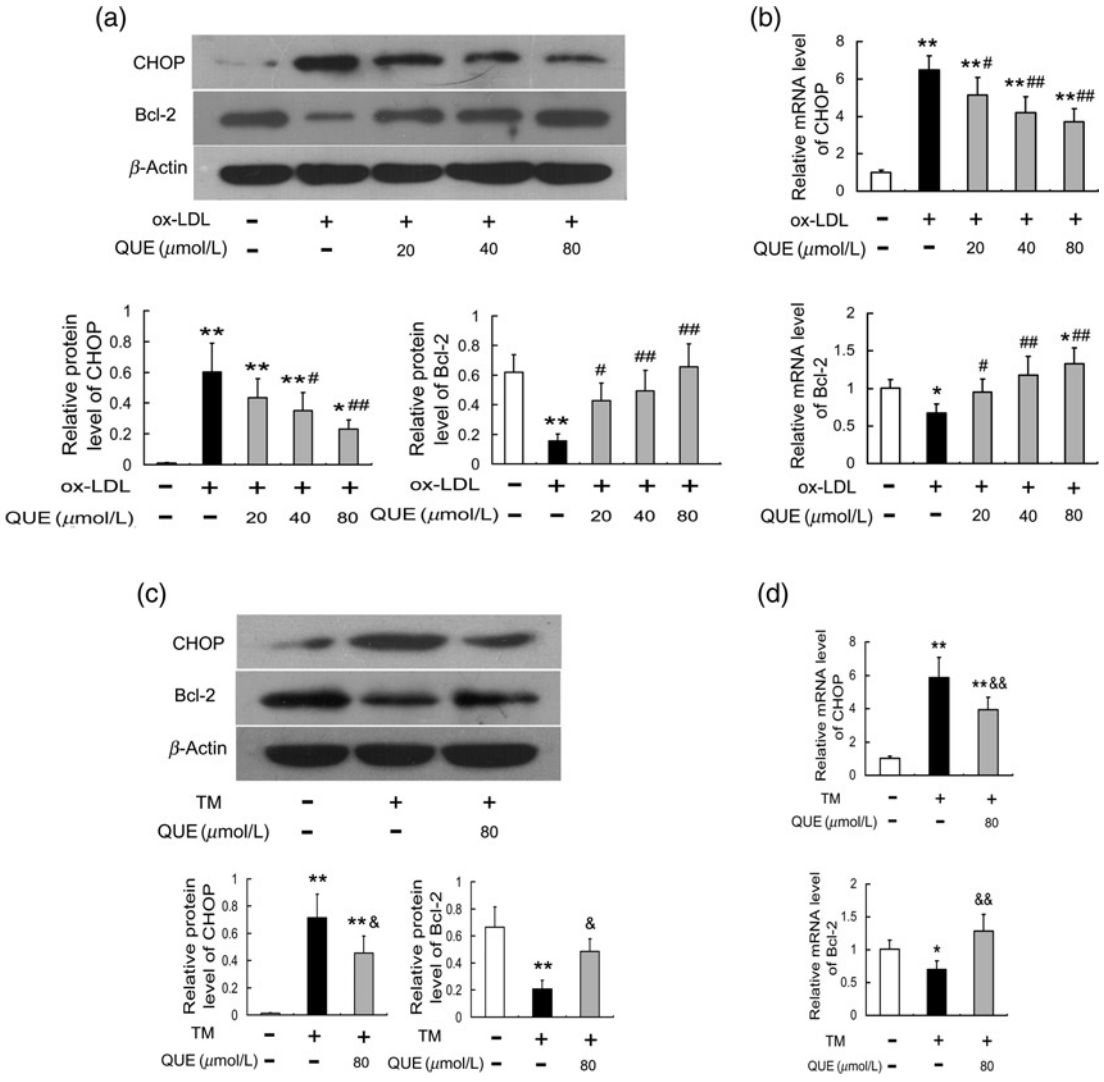

Figure 4 Effect of QUE on CHOP and Bcl-2 expression induced by ox-LDL or tunicamycin (TM) in RAW264.7 cells. Cells were treated as described in Figure 3. The expression of CHOP and Bcl-2 were analyzed by Western blot and normalized to β-actin levels (a and c). The mRNA levels of CHOP and Bcl-2 were measured by quantitative realtime PCR, which were measured relative to time-matched, vehicle-treated controls and calculated after adjusting for β-actin using the $2^{-\Delta\Delta Ct}$ method (b and d). Data are presented as the mean $\pm$ SEM of at least three independent experiments. $^{*}P < 0.05$, $^{**}P < 0.01$ versus vehicle-treated control; $^{\#}P < 0.05$, $^{\#\#}P < 0.01$ versus ox-LDL treatment; $^{\&}P < 0.05$, $^{\&\&}P < 0.01$ versus TM treatment. QUE, quercetin; ox-LDL; oxidized LDL; CHOP, C/EBP homologous protein

Increasing evidence strongly suggests that ox-LDL causes apoptosis and necrosis of macrophages.[32] Ox-LDL is taken up by scavenger receptors on macrophages and results in a large accumulation of cholesterol in macrophages, which results in disruption of lipid homeostasis. Furthermore, cellular accumulation of excess cholesterol may serve as a trigger for cell death, which then promotes artery intimal inflammation, calcification, thrombosis and plaque rupture, which are the major sequelae of advanced atherosclerosis.[33] QUE has been shown to protect cultured macrophages from apoptosis induced by H_2O_2.[14] However, whether QUE could inhibit macrophage-derived foam cell formation and protect macrophages against ox-LDL-induced apoptosis had not yet been studied. Our data demonstrated that macrophages treated with ox-LDL for 24 h accumulated significant amounts of lipid as measured by oil red O staining and intracellular TC assay, with a concomitant increase in the apoptotic rate of cells. In contrast, addition of QUE to ox-LDL-treated macrophages reduced the ox-LDL uptake by RAW264.7 cells and decreased the apoptotic rate in a dose-dependent manner.

The protective effects of QUE have been observed in different cell types, but the mechanism is not completely understood. Suematsu *et al.*[34] indicated that QUE was able to inhibit H_2O_2-induced apoptosis in neuronal SH-SY5Y cells by inhibiting the pro-apoptotic Bax gene expression, enhancing the antiapoptotic Bcl-2 gene expression and inhibiting the activation of the caspase cascade. Wang *et al.*[35] indicated that the antiapoptotic effect of QUE is via the activation of the PI3K/Akt signaling pathway. Chow *et al.*[14] demonstrated that the antioxidant potential of QUE might contribute to the protective effect of QUE on H_2O_2-induced apoptosis in macrophage cells. In contrast, QUE has also been shown to induce apoptosis by activating

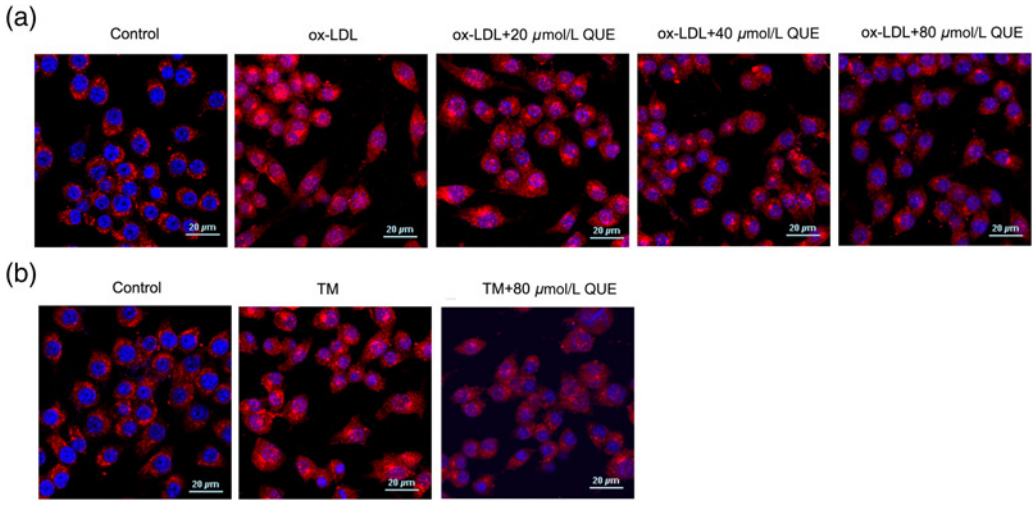

Figure 5 QUE inhibits nuclear translocation of ATF6 in RAW264.7 macrophages. Cells were treated as described in Figure 3. Immunofluorescence experiments show ATF6 visualized by Cy3 labeling (red) and nuclei stained with DAPI (blue) with laser scanning confocal microscope. Representative fluorescent images are shown. Scale bar = 20 μm. DAPI, 4′,6-diamidino-2-phenylindole; ATF6, activating transcription factor 6; QUE, quercetin; ox-LDL; oxidized LDL. (A color version of this figure is available in the online journal)

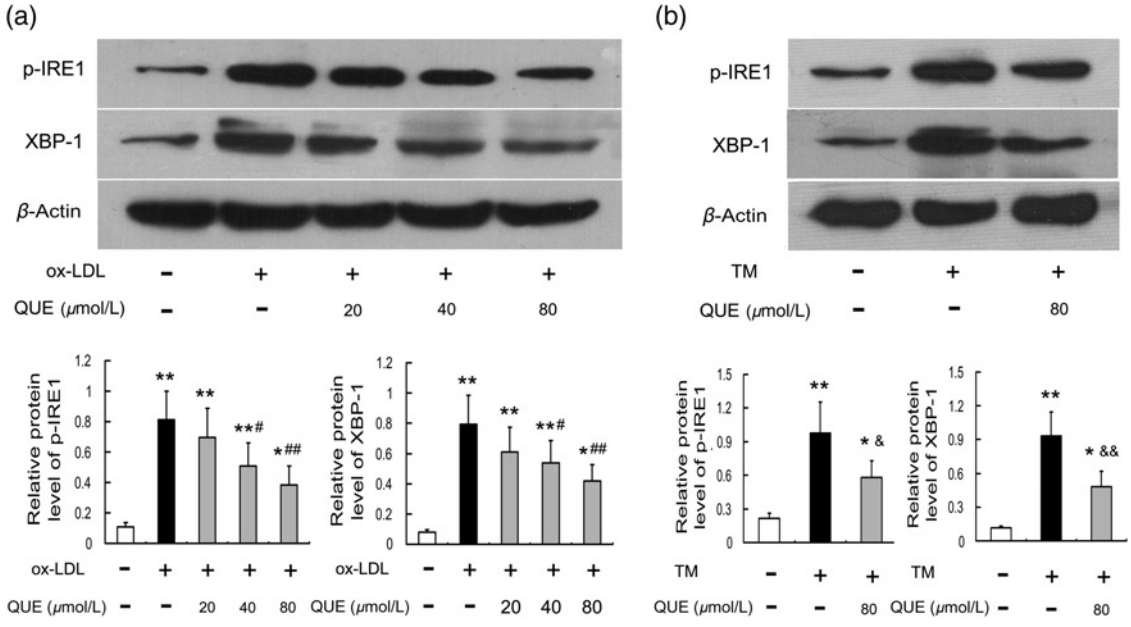

Figure 6 QUE inhibits the upregulation of p-IRE1 and XBP-1 expression induced by ox-LDL or tunicamycin (TM) in RAW264.7 cells. Cells were treated as described in Figure 3. The expression of p-IRE1 and XBP-1 proteins was analyzed by Western blot, and the protein concentrations were normalized to β-actin proteins levels (a and b). Data are expressed as the mean ± SEM of at least three independent experiments. $^{*}P < 0.05$, $^{**}P < 0.01$ versus vehicle-treated control; $^{\#}P < 0.05$, $^{\#\#}P < 0.01$ versus ox-LDL treatment; $^{\&}P < 0.05$, $^{\&\&}P < 0.01$ versus TM treatment. QUE, quercetin; ox-LDL; oxidized LDL; p-IRE1, phospho-inositol-requiring enzyme 1; XBP-1, X-box-binding protein 1

the mitochondria-dependent pathway in cancer cells.[36,37] Therefore, the biological effects of QUE in cells are controversial and require further elucidation. In this study, we found that QUE downregulated CHOP expression by inhibiting ATF6 activation and IRE1 phosphorylation and inhibited ox-LDL-induced apoptosis in RAW264.7 cells. TM has been known to promote apoptosis by activating ER stress signaling pathways.[38] Therefore, we further examined the effect of QUE on TM-induced apoptosis in RAW264.7 cells. We found that QUE attenuated TM-induced cytotoxicity with a decrease in CHOP expression. The activation of ATF6 and IRE1 induced by TM was also significantly suppressed by QUE. This suggested that suppression of the ER stress-CHOP pathway by QUE is involved in the prevention of ox-LDL-induced apoptosis.

ER is an organelle present in all eukaryotic cells and plays a leading role in protein synthesis and regulation of calcium homeostasis. However, the ER is sensitive to multiple stimuli, such as oxidative stress, dysregulation of calcium dynamics, inhibition of sugar chain modification and so on, which lead to ER dysfunction characterized by the accumulation of unfolded and/or misfolded proteins and

an imbalance in calcium homeostasis (ER stress).[39] It is well known that ER stress is an adaptive mechanism by which cells react to perturbations in ER homeostasis through translational attenuation and the upregulation of ER chaperone genes and related proteins. However, when ER function is severely impaired, the organelle triggers apoptotic signals. One component of the ER stress-mediated apoptosis pathway is CHOP.[16–21] CHOP knockout mice show normal development and fertility but exhibit reduced apoptosis in response to ER stress.[20] Thus, the induction of CHOP indicates an increase in ER-initiated apoptosis. Although the direct transcriptional target of CHOP has not been found,[40] the Bcl-2 pathway may be involved downstream of CHOP, thereby connecting CHOP activation and apoptosis.[26,41] Members of the Bcl-2 family are also located on the ER, and Bcl-2 plays a central role in regulating pathways that are anti-apoptotic. In this study, we showed that ox-LDL or TM treatment increased the expression of CHOP and decreased Bcl-2 expression in RAW264.7 cells, and these alterations were significantly inhibited by QUE.

ATF6 and IRE1 are two important upstream molecules that play an important role in the induction of CHOP in ER stress. ATF6 is a type II transmembrane protein, and its intra-ER domain is linked to glucose-regulated proteins 78 (GRP78), resulting in the physiological inactivation of ATF6. Under conditions of increased ER stress, ATF6 dissociates from GRP78, translocates to the Golgi apparatus and is processed by site 1 protease or site 2 protease. Processed ATF6 translocates to the nucleus and upregulates target genes such as CHOP via the ER stress response element (ERSE).[27,28,42] IRE1 is a type I transmembrane protein with kinase and endonuclease activities. Under conditions of increased ER stress, its endonuclease activity is triggered by oligomerization and auto-phosphorylation. This leads to the catalytic removal of a 26-bp intron from the mRNA of XBP-1, and mature XBP-1 mRNA is translated into the transcription factor that regulates the expression of target genes like CHOP, also via the ERSE.[29,30] This study showed that similar to TM, ox-LDL had an effect that resulted in the translocation of ATF6 from the cytoplasm into the nucleus and upregulation of p-IRE1 and XBP1, and this effect was significantly suppressed when RAW264.7 cells were pharmacologically treated with QUE.

In conclusion, this study showed for the first time that a natural product, quercetin, protected RAW264.7 macrophage cells from ox-LDL-induced apoptosis through the inhibition of the ER stress-CHOP pathway *in vitro*. These results might explain the diverse physiological activities of quercetin and shed light on the pharmacological application of quercetin in atherosclerosis-related diseases.

Authors contributions: SY carried out the study design, data collection and analysis, the cell studies and drafted the manuscript. HS helped to carry out oil red O staining. GS and NY helped to carry out Western blot analysis and immunofluorescence assay. QL helped to prepare ox-LDL. PJ helped to perform flow cytometry analysis. YZ and CZ participated in the cell studies. SQ was responsible for the study design, the funding, the data analysis and the manuscript draft. All authors read and approved the final manuscript.

ACKNOWLEDGEMENTS

This research was supported by the Taishan Scholars Foundation of the Shandong Province (zd056, zd057), National Natural Science Foundation of China (30971098) and Natural Science Foundation of Taishan Medical University (2011ZR038). We also thank the colleagues in our laboratory for their discussion and support.

REFERENCES

1 Shin J, Edelberg JE, Hong MK. Vulnerable atherosclerotic plaque: clinical implications. *Curr Vasc Pharmacol* 2003;**1**:183–204
2 Tabas I. Consequences and therapeutic implications of macrophage apoptosis in atherosclerosis: the importance of lesion stage and phagocytic efficiency. *Arterioscler Thromb Vasc Biol* 2005;**25**:2255–64
3 Seimon T, Tabas I. Mechanisms and consequences of macrophage apoptosis in atherosclerosis. *J Lipid Res* 2009;**50**:S382–7
4 Tabas I. Apoptosis and plaque destabilization in atherosclerosis: the role of macrophage apoptosis induced by cholesterol. *Cell Death Differ* 2004;**11**:S12–6
5 Liu J, Thewke DP, Su YR, Linton MF, Fazio S, Sinensky MS. Reduced macrophage apoptosis is associated with accelerated atherosclerosis in low-density lipoprotein receptor-null mice. *Arterioscler Thromb Vasc Biol* 2005;**25**:174–9
6 Tiwari RL, Singh V, Barthwal MK. Macrophages: an elusive yet emerging therapeutic target of atherosclerosis. *Med Res Rev* 2008;**28**:483–544
7 Perez-Vizcaino F, Duarte J. Flavonols and cardiovascular disease. *Mol Aspects Med* 2010;**31**:478–94
8 Ben Abdallah F, Zribi N, Ammar-Keskes L. Antioxidative potential of quercetin against hydrogen peroxide induced oxidative stress in spermatozoa in vitro. *Andrologia* 2011;**43**:261–5
9 Mackraj I, Govender T, Ramesar S. The antihypertensive effects of quercetin in a salt-sensitive model of hypertension. *J Cardiovasc Pharmacol* 2008;**51**:239–45
10 Rivera L, Morón R, Sánchez M, Zarzuelo A, Galisteo M. Quercetin ameliorates metabolic syndrome and improves the inflammatory status in obese Zucker rats. *Obesity (Silver Spring)* 2008;**16**:2081–7
11 Zhang ZJ, Cheang LC, Wang MW, Lee SM. Quercetin exerts a neuroprotective effect through inhibition of the iNOS/NO system and pro-inflammation gene expression in PC12 cells and in zebrafish. *Int J Mol Med* 2011;**27**:195–203
12 Mojzisová G, Sarisský M, Mirossay L, Martinka P, Mojzis J. Effect of flavonoids on daunorubicin-induced toxicity in H9c2 cardiomyoblasts. *Phytother Res* 2009;**23**:136–9
13 Choi JS, Kang SW, Li J, Kim JL, Bae JY, Kim DS, Shin SY, Jun JG, Wang MH, Kang YH. Blockade of oxidized LDL-triggered endothelial apoptosis by quercetin and rutin through differential signaling pathways involving JAK2. *J Agric Food Chem* 2009;**57**:2079–86
14 Chow JM, Shen SC, Huan SK, Lin HY, Chen YC. Quercetin, but not rutin and quercitrin, prevention of H_2O_2-induced apoptosis via anti-oxidant activity and heme oxygenase 1 gene expression in macrophages. *Biochem Pharmacol* 2005;**69**:1839–51
15 Gargalovic PS. Atherogenesis on the chopping block. *Cell Metab* 2009;**9**:399–401
16 Miyazaki Y, Kaikita K, Endo M, Horio E, Miura M, Tsujita K, Hokimoto S, Yamamuro M, Iwawaki T, Gotoh T, Ogawa H, Oike Y. C/EBP homologous protein deficiency attenuates myocardial reperfusion injury by inhibiting myocardial apoptosis and inflammation. *Arterioscler Thromb Vasc Biol* 2011;**31**:1124–32
17 Song B, Scheuner D, Ron D, Pennathur S, Kaufman R. Chop deletion reduces oxidative stress, improves beta cell function, and promotes cell survival in multiple mouse models of diabetes. *J Clin Invest* 2008;**118**:3378–89
18 Tsukano H, Gotoh T, Endo M, Miyata K, Tazume H, Kadomatsu T, Yano M, Iwawaki T, Kohno K, Araki K, Mizuta H, Oike Y. The endoplasmic

reticulum stress-C/EBP homologous protein pathway-mediated apoptosis in macrophages contributes to the instability of atherosclerotic plaques. *Arterioscler Thromb Vasc Biol* 2010;**30**:1925–32
19 Devries-Seimon T, Li Y, Yao PM, Stone E, Wang Y, Davis RJ, Flavell R, Tabas I. Cholesterol-induced macrophage apoptosis requires ER stress pathways and engagement of the type A scavenger receptor. *J Cell Biol* 2005;**171**:61–73
20 Feng B, Yao PM, Li Y, Devlin CM, Zhang D, Harding HP, Sweeney M, Rong JX, Kuriakose G, Fisher EA, Marks AR, Ron D, Tabas I. The endoplasmic reticulum is the site of cholesterol-induced cytotoxicity in macrophages. *Nat Cell Biol* 2003;**5**:781–92
21 Thorp E, Li G, Seimon TA, Kuriakose G, Ron D, Tabas I. Reduced apoptosis and plaque necrosis in advanced atherosclerotic lesions of Apoe-/- and Ldlr-/- mice lacking CHOP. *Cell Metab* 2009;**9**: 474–81
22 Myoishi M, Hao H, Minamino T, Watanabe K, Nishihira K, Hatakeyama K, Asada Y, Okada K, Ishibashi-Ueda H, Gabbiani G, Bochaton-Piallat ML, Mochizuki N, Kitakaze M. Increased endoplasmic reticulum stress in atherosclerotic plaques associated with acute coronary syndrome. *Circulation* 2007;**116**:1226–33
23 Martinet W, Kockx MM. Apoptosis in atherosclerosis: focus on oxidized lipids and inflammation. *Curr Opin Lipidol* 2001;**12**:535–41
24 Yao ST, Sang H, Yang NN, Kang L, Tian H, Zhang Y, Song GH, Qin SC. Oxidative low density lipoprotein induces macrophage ER stress via CD 36. *Sheng Li Xue Bao* 2010;**62**:433–40
25 Boullier A, Li Y, Quehenberger O, Palinski W, Tabas I, Witztum JL, Miller YI. Minimally oxidized LDL offsets the apoptotic effects of extensively oxidized LDL and free cholesterol in macrophages. *Arterioscler Thromb Vasc Biol* 2006;**26**:1169–76
26 McCullough KD, Martindale JL, Klotz LO, Aw TY, Holbrook NJ. Gadd153 sensitizes cells to endoplasmic reticulum stress by down-regulating Bcl-2 and perturbing the cellular redox state. *Mol Cell Biol* 2001;**21**:1249–59
27 Horibe T, Hoogenraad NJ. The chop gene contains an element for the positive regulation of the mitochondrial unfolded protein response. *PLoS One* 2007;**2**:e835
28 Yoshida H, Okada T, Haze K, Yanagi H, Yura T, Negishi M, Mori K. ATF6 activated by proteolysis binds in the presence of NF-Y (CBF) directly to the cis-acting element responsible for the mammalian unfolded protein response. *Mol Cell Biol* 2000;**20**:6755–67
29 Tsutsumi S, Gotoh T, Tomisato W, Mima S, Hoshino T, Hwang HJ, Takenaka H, Tsuchiya T, Mori M, Mizushima T. Endoplasmic reticulum stress response is involved in nonsteroidal anti-inflammatory drug-induced apoptosis. *Cell Death Differ* 2004;**11**:1009–16
30 Yoshida H, Matsui T, Yamamoto A, Okada T, Mori K. XBP1 mRNA is induced by ATF6 and spliced by IRE1 in response to ER stress to produce a highly active transcription factor. *Cell* 2001;**107**:881–91
31 Stoneman VE, Bennett MR. Role of apoptosis in atherosclerosis and its therapeutic implications. *Clin Sci* 2004;**107**:343–54
32 Wintergerst ES, Jelk J, Rahner C, Asmis R. Apoptosis induced by oxidized low density lipoprotein in human monocyte-derived macrophages involves CD36 and activation of caspase-3. *Eur J Biochem* 2000;**267**:6050–9
33 Tabas I. Consequences of cellular cholesterol accumulation: basic concepts and physiological implications. *J Clin Invest* 2002;**110**:905–11
34 Suematsu N, Hosoda M, Fujimori K. Protective effects of quercetin against hydrogen peroxide-induced apoptosis in human neuronal SH-SY5Y cells. *Neurosci Lett* 2011;**504**:223–7
35 Wang XQ, Yao RQ, Liu X, Huang JJ, Qi DS, Yang LH. Quercetin protects oligodendrocyte precursor cells from oxygen/glucose deprivation injury in vitro via the activation of the PI3K/Akt signaling pathway. *Brain Res Bull* 2011;**86**:277–84
36 Liang W, Li X, Li C, Liao L, Gao B, Gan H, Yang Z, Liao L, Chen X. Quercetin-mediated apoptosis via activation of the mitochondrial-dependent pathway in MG-63 osteosarcoma cells. *Mol Med Rep* 2011;**4**:1017–23
37 Xie X, Yin J, Jia Q, Wang J, Zou C, Brewer KJ, Colombo C, Wang Y, Huang G, Shen J. Quercetin induces apoptosis in the methotrexate-resistant osteosarcoma cell line U2-OS/MTX300 via mitochondrial dysfunction and dephosphorylation of Akt. *Oncol Rep* 2011;**26**:687–93
38 Kim KH, Gao Y, Walder K, Collier GR, Skelton J, Kissebah AH. SEPS1 protects RAW264.7 cells from pharmacological ER stress agent-induced apoptosis. *Biochem Biophys Res Commun* 2007;**354**:127–32
39 Hotamisligil GS. Endoplasmic reticulum stress and atherosclerosis. *Nat Med* 2010;**16**:396–9
40 Oyadomari S, Mori M. Roles of CHOP/GADD153 in endoplasmic reticulum stress. *Cell Death Differ* 2004;**11**:381–9
41 Pedruzzi E, Guichard C, Ollivier V, Driss F, Fay M, Prunet C, Marie JC, Pouzet C, Samadi M, Elbim C, O'Dowd Y, Bens M, Vandewalle A, Gougerot-Pocidalo MA, Lizard G, Ogier-Denis E. NAD(P)H oxidase Nox-4 mediates 7-ketocholesterol-induced endoplasmic reticulum stress and apoptosis in human aortic smooth muscle cells. *Mol Cell Biol* 2004;**24**:10703–17
42 Adachi Y, Yamamoto K, Okada T, Yoshida H, Harada A, Mori K. ATF6 is a transcription factor specializing in the regulation of quality control proteins in the endoplasmic reticulum. *Cell Struct Funct* 2008;**33**:75–89

(Received January 19, 2011, Accepted March 14, 2012)